

EBERHARD KARLS
UNIVERSITÄT
TÜBINGEN



Fast Dose Estimation for Radiotherapy Treatment Plans with Uncertainty Estimation

Master Thesis

supervised by
Prof. Dr. Daniela Thorwarth and Dr. Christian
Baumgartner

Simon Gutwein

October 19, 2021

Aufbau

Abstract

- Klassisches Abstract

Dedication

- Klassische Dedication

Declaration

- Klassische Declaration (schauen ob es von Tübingen eine Vorlage gibt)

Introduction

- Was ist Radiotherapy und warum ist die so interessant
- Wie läuft eine Radiotherapy ab
- Worauf kommt es bei der Radiotherapy drauf an
- Was ist der limitierende Faktor bei Monte Carlo
- Was ist Machine Learning und warum ist es von Interesse

Previous Work

- Work that proposes a different method to solve the same problem.
- Work that uses the same proposed method to solve a different problem.
- A method that is similar to your method that solves a similar problem.
- A discussion of a set of related problems that covers your problem domain.

Material & Methods // Proposed Method

- Worauf baue ich auf (DeepDose)
- Baseline Experiment
- Testen gegen Baseline
- Wie erweitere ich dieses Modell:
- RevNet (Christan Baumgartner), Uncertainty Estimation

Results

- Performance Ergebnisse des Baseline Netzwerks
- Performancewerte für unterschiedliche Entitäten
- Performance Werte mit RevNet
- Funktioniert die quantifizierung der Uncertainty mit dem Ansatz

Discussion

- Wie sind unsere Ergebnisse einzuordnen im Vergleich zu der Baseline
- Netzwerk Performance bei der unterschiedlichen Entitäten
- Welchen Impact hat das Training mit neuen Entitäten
- Welchen Impact hat das Training mit größeren Patches (s. RevNet)
- Wie funktioniert die Uncertainty Quantification
- Was sind die Limitationen

Dedication

Lorem ipsum dolor sit amet, consetetur sadipscing elitr, sed diam nonumy eirmod tempor invidunt ut labore et dolore magna aliquyam erat, sed diam voluptua. At vero eos et accusam et justo duo dolores et ea rebum. Stet clita kasd gubergren, no sea takimata sanctus est Lorem ipsum dolor sit amet. Lorem ipsum dolor sit amet, consetetur sadipscing elitr, sed diam nonumy eirmod tempor invidunt ut labore et dolore magna aliquyam erat, sed diam voluptua. At vero eos et accusam et justo duo dolores et ea rebum. Stet clita kasd gubergren, no sea takimata sanctus est Lorem ipsum dolor sit amet.

Declaration

I hereby declare that I have written the submitted Master's thesis without outside help. I have marked as such all statements taken verbatim or in spirit from other works, if applicable also from electronic media. I am aware that my Master's thesis in digital form will be checked for plagiarism if unmarked texts are used in whole or in part. A violation of the basic rules of scientific work is considered as an attempt to deceive or cheat and will result in the corresponding consequences according to the valid examination regulations of the Medical Radiation Sciences degree programme. For the purpose of comparing my Master's thesis with existing sources, I agree that my Master's thesis will be entered into a database where it will remain after my graduation. I do not cede any further rights to reprint and use it. I further declare that the thesis has not been the subject of any other examination procedure, neither in its entirety nor in essential parts, and that it has not been published.

Signature

Date

Contents

1	Aufbau	1
2	Dedication	3
3	Declaration	4
4	Introduction	8
5	Material & Methods	12
6	Results	19
7	Discussion	20
8	Conclusion	21
A	Appendix Title	26

List of Figures

5.1	3D U-Net architecture	13
5.2	Performance of the networks, trained on mixed and on prostate only patients anatomies and plan configurations. The underlying bar chart (left y axis) shows the occurneces of the fieldsizes listed on the x axis. The box plots (right y axis) shows the performance value of each discretized fieldsize range for both mixed and prostate only trained model. Outliers are depicted with a diamond shape	13
5.3	NONE	14
5.4	NONE	14
5.5	NONE	15
5.6	NONE	15
5.7	Sample from a slice of training data. From left to right: beam shape, CT with Hounsfield Units, radiological depth, center beamline distance, source distance	16
5.8	Dataloading scheme	17

List of Tables

5.1 Settings used for gamma analysis of single segments and entire radiation plans. 18

Introduction

Introduction

- **Genereller Ablauf am MR-Linac stand jetzt**
- Person kommt, bekommt ein CT für initiale Planung, danach wird dann bei Bestrahlung des Patienten ein MRT von dem Patienten gemacht. Registrierung von CT und MRT und adaption von contours auf MRT. Dann Online-Plan adaption bei dem Plan aufgrund von adapt to position oder shape. Results in no adaption or adaption of segments shape, monitor units or both. This is repeated for each treatment fraction of the patient (Adaptive radiotherapy: The Elekta Unity MR-linac concept)
- **Wie soll der Ablauf einmal aussehen beim MR-Linac**
- Goal is to achieve a MRI-only treatment workflow, including imaging with MRI contouring on MRI and planning and calculation of plans on mri. dose calculation is not possible on mri data because mri is not a quantitative imaging modality, meaning pixel values give no information about the electron density of the underlying tissue or body part. therefore synthetic ct images need to be created from mri images, which enable dose calculations.
- **Und dann auf Dosisdeposition eingehen / Was ist aktuelle Methode** hier noch viel verschieben nach material und methodik
- (<http://dx.doi.org/10.1118/1.2795842>) monte carlo simulations are currently used for dose calculation for radiotreatment plans in a clinical setting. The interactions of photons in human tissue in the energy spectrum of interest for external beam therapy transfer the photon energy on to electrons or positrons. these particles then transfer their energy into the surrounding tissue. before energy deposition the photon and especially the electron undergo a number of elastic and non elastic interactions with atoms. In the process the main energy loss is caused by inelastic collisions and radiative interactions. the collisions result in ionization and therefore secondary electrons. radiative interactions result in a energy transfer back to photons. the sum of these phenomena in a photon field results in a coupled electron-photon shower, which can be described by a coupled set of integrodifferential transport equations. due to the lack of a analytical solution, without any major simplifications and assumptions for conditions, the monte carlo algorithm is used to simulate a multitude of particle histories in the desired target volume. partial histories describe the exact way of a photon from the source to its point in the volume where it has lost all of its energy including energy transport to secondary

electrons in the process of collisions. the stochastic nature of the interaction processes of photons and electrons need for a large number of simulated particles to achieve an accurate result of dose deposition. the entirety of all simulated particles then results in an accurate dose distribution which can be used for treatment planning. the need for particle histories in the magnitude of 10^7 to 10^{11} for accurate dose estimations, result in long simulation times.

- Wo findet Deep Learning Anwendung (Bezug zu Medizin)
- Deep learning and especially computer vision is already present in current research of Biology, Physics as well as medicine. there are a multiple fields in which CV can be applied to fields such as dermatology (<https://sci-hub.ru/10.1038/nature21056>), radiology (<https://sci-hub.ru/10.1038/srep24454>, <https://sci-hub.ru/10.1097/rli.0000000000000341>), cardiology (<https://arxiv.org/abs/1708.09843>) or pathology (<https://www.nature.com/articles/s41598-020-58467-9.pdf>)
- Einleitung zu Deep Learning
- . deep learning is a preferred tool due to its short inference times as well as super human performance level on certain tasks. the implementation of the fully convolutional network (<https://arxiv.org/pdf/1411.4038.pdf>) and its further development of the U-Net utilizing data from higher level representations of the data in the form of skip connections (<https://arxiv.org/abs/1505.04597>) have revolutionized the application of deep learning for image data and 3d data in the form of a 3D-UNets.
- Was ist die Contribution / Aims <- Ziel: Dosisvorhersage mit DL, möglichst robust
- In this paper we investigate the capabilities of deep learning in the field of dose predictions for radio treatment plans. we aimed to achieve a robust dose prediction irrespective of the body region of interest and irrespective of the complexity of the treatment plan.
-

Show why Radiotherapy is so important: search for sources of application of radiotherapy for different entities. Prostate: [1, 2, 3] Mamma: [4, 5, 6] Head & Neck: [7, 8, 9, 10] Liver: [11, 12, 13, 14, 15] Lymph Nodes: [16, 17, 18, 19, 20]

Was ich noch brauche: Infos über MR-Linac, was ist die Vision hinter dem MR Linac (online adaption)

The use of Magnet Resonance Imaging (MRI) during radiotherapy has opened a variety of new opportunities for treatment optimization. MRI provides a better contrast in soft tissue areas of the body, compared to conventional computed tomography (CT), and can be used to assess functional image data from the patient

in real time. The enhanced contrast leads to better organs at risk (OAR) and tumor volume delineation. (doi:10.1016/S0360-3016(03)01446-9). Recent research efforts are exploring the capabilities of the hybrid MRI linear accelerator (MRI-Linac) (doi:10.1007/s00066-018-1386-z, doi:10.1016/j.radonc.2007.10.034, doi:10.1002/acm2.12233). The introduction of the MRI-Linac has transformed the clinical workflow for radiotherapy as well as treatment planning. Patients are required to receive one CT for initial treatment planning. For radiation in each fraction, the initial plan is registered on the current MRI and optionally adapted to shift or size variation of the tumor volume (doi:10.1016/j.ctro.2019.04.001). Goal is to reach an MRI-only-workflow where image acquisition, treatment planning and radiotherapy only involve the MRI-Linac. To achieve this goal multiple steps in the clinical workflow need to be adapted

behind MRI Linac is an radiotreatment adaption in an online manner, meaning that a shift of the tumor volume and changes to the patients anatomy due to movement can be considered to adapt the treatmentplan. This results in smaller safety margins (doi:10.1102/1470-7330.2004.0054) for tumor volumes and ultimately result in a lower delivered dose to organs at risk. To achieve this ultimate goal, multiple steps, such as anatomy segmentation, treatmentplan adaption and dose deposition simulations need to be able to be performed in real-time.

Welche Besonderheiten gibt es bei einem MR-Linac im Vergleich zu einem normalem Bestrahlter (Stichworte: ERE, Electron Deposition Shift) Wie funktioniert normale Dosisberechnung (Monte Carlo doi:10.1118/1.598917), warum ist der Nutzen davon limitiert wenn man in die online Adaption möchte.

However, since MC simulation is a stochastic process, the resulting dose map contains inherent quantum noise whose variance is inversely proportional to the number of the simulation histories and, accordingly, to the simulation time. Typically, achieving clinically acceptable precision requires hours of CPU computation time. Graphics processing unit (GPU)-based parallel computation frameworks can accelerate MC simulation to a few minutes for a typical IMRT/VMAT plan (doi:10.1088/0031-9155/55/11/006)

However, several areas in the clinical workflow require real-time dose calculation, such as inverse optimization of the treatment planning process for IMRT and VMAT (doi:10.1088/2632-2153/abdbfe) especially online radiotherapy and online plan adaption are limited by the time needed to recalculate dose distributions of beam settings and patient anatomies due to moving organs (doi:10.1016/j.clon.2018.08.001)

Machine Learning Teil: Wie wird Machine Learning in verschiedenen Bereichen der Bestrahlungsplanung bezüglich MRI genutzt: Eine Implementierung und Nutzung dieser könnte zum Erreichen einer Online-Bestrahlungsadaption führen

1. Autosegmentation ([21, 22]) as well as uncertainty ([23])
2. Radio Treatment Plan optimization ([24, 25])

3. Dose Estimation ([26, 27] active denoising of lower history MC Simulations (doi:10.1002/mp.13856))
4. Pseudo CT ([28, 29, 30])

Material & Methods

Patient Data

We used the treatment information from 45 prostate, 10 breast, 10 lymph node, 10 head and neck and 10 liver patients who were previously treated using the MRI-Linac Elekta Unity (Elekta, Stockholm, Sweden) in our institution. **List fieldsizes, and gantry angle distribution (maybe a fanfy plot with a circular coordinate system, like a distribution over angles) respectively.** To to improve transational capabilities of the network

List how many segments for which entity I used and then how i split them up into training, validation and test patients and their respective number of segments. to match CT image shape dose distribution were resized to match the 512x512x number of slices shape of the ct input array. (siehe workflow_code/utlis.py skripte). The original iso center of the plan was used weather it was centered in the volume or not.

Ground truth dose distributions were calculated EGSnrc using 10^7 histories. (information über EGSnrc also software version und release [31]) Each segment was calculated using same number of monitor units which enabled me to scale the segment based on the segment weight when predicting an entire treatment plan.

Network

The U-Net expects a 3d input of size (batchsize, num_masks, W, H, D) and samples this input over the encoding path down to extract important features on a lower level scale from size [W, H, D] down to [W/2, H/2, D/2]. The decoding is done using 3D transposed convolutions with a kernel size and a stride of 2 respectively. A skip connecting was added to before pooling to pass on higher level of volume resolution to later parts of the U-Net. Each block building block consists of a convolutional layer with zero padding, to maintain dimensionality, kernel size 3x3x3 and a stride of 1, a 3D batch normalization layer and a ReLU layer. No dropout was used. Modified version of (doi:10.1007/978-3-319-24574-4_28)

Input Data

The input of the network consists of 5 different masks containig spatial information about the given volume. (insert image with different masks and a little description of it) refer to deepdose paper by kontaxis [26]

in the image above the the different input masks can bee seen. the masks are the binary beam shape (a), ct image with (electron density oder HU values, mal

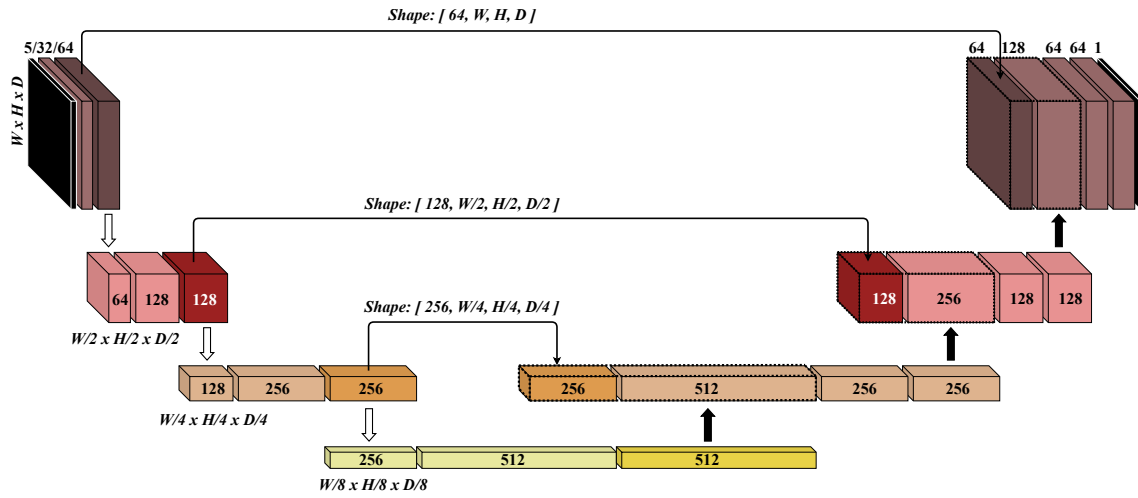


Figure 5.1: 3D U-Net architecture

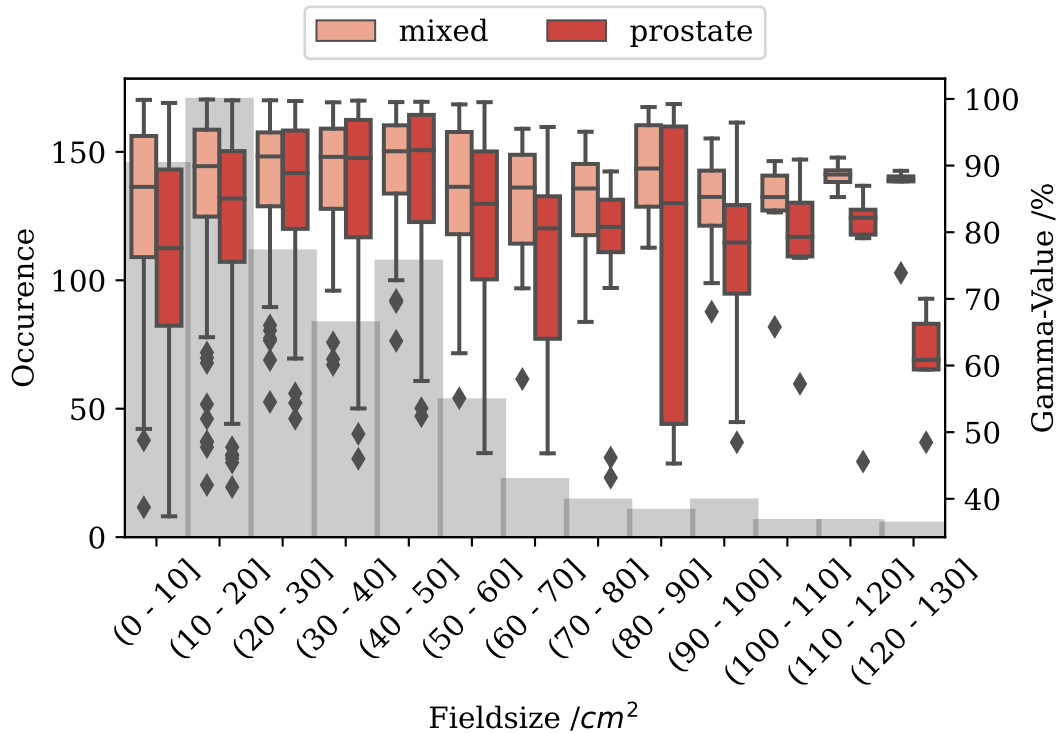


Figure 5.2: Performance of the networks, trained on mixed and on prostate only patients anatomies and plan configurations. The underlying bar chart (left y axis) shows the occurnces of the fieldsizes listed on the x axis. The box plots (right y axis) shows the performance value of each discretized fieldsize range for both mixed and prostate only trained model. Outliers are depicted with a diamond shape

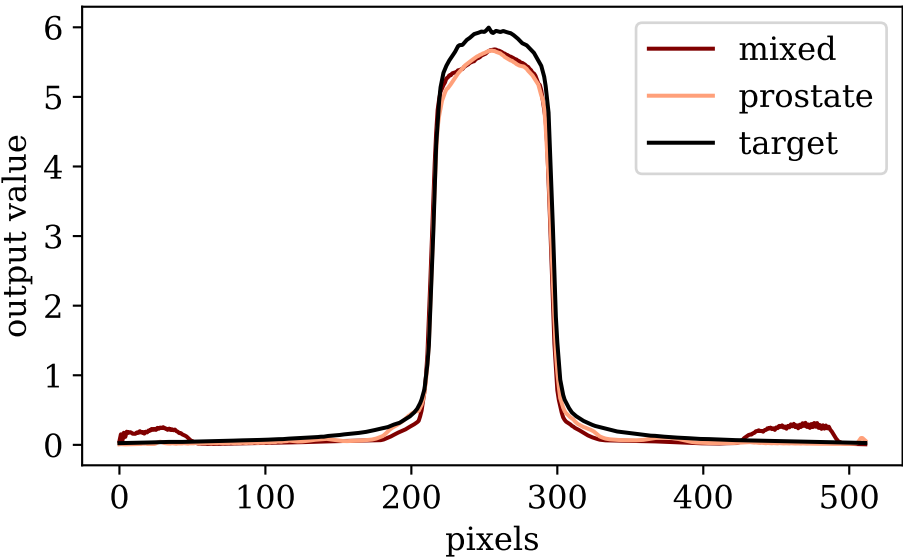


Figure 5.3: NONE

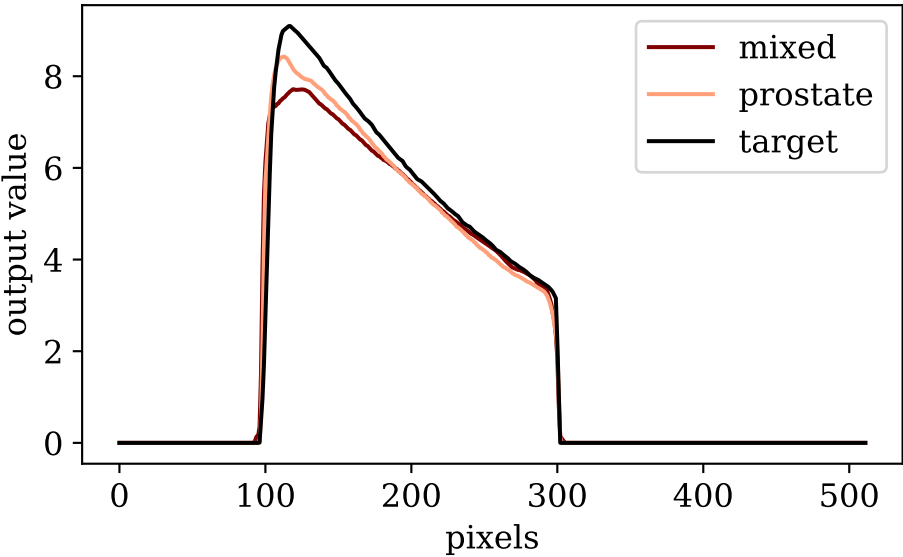


Figure 5.4: NONE

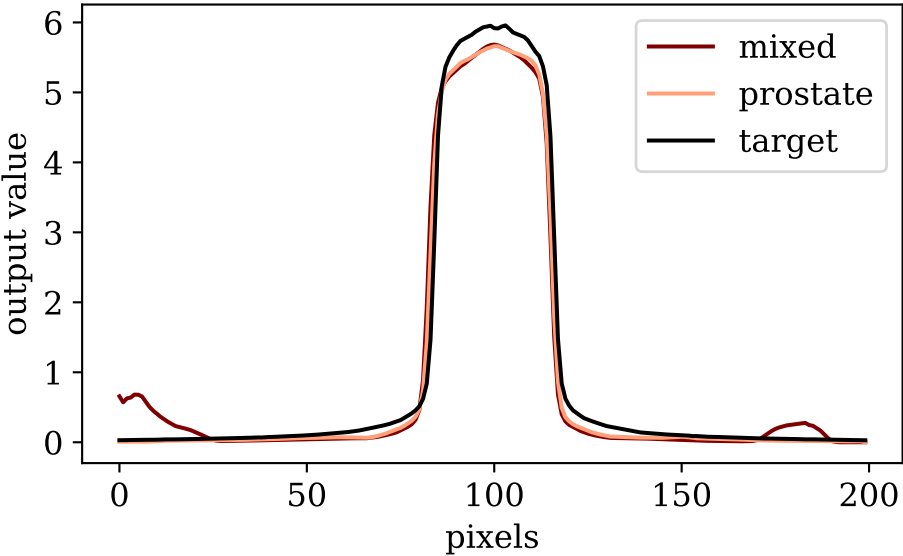


Figure 5.5: NONE

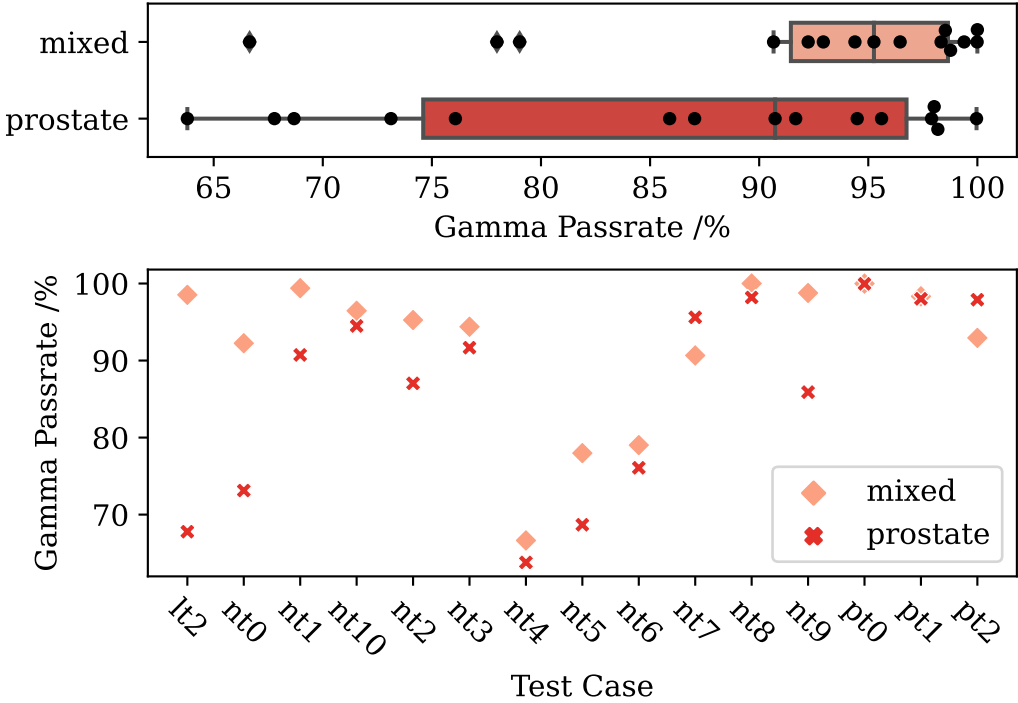


Figure 5.6: NONE

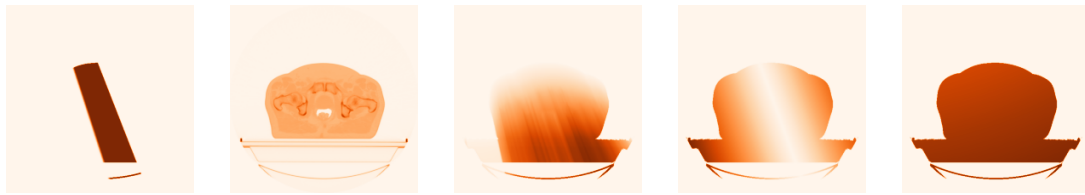


Figure 5.7: Sample from a slice of training data. From left to right: beam shape, CT with Hounsfield Units, radiological depth, center beamline distance, source distance

schaufen was besser performed) (b) radiological depth (c) center beamline distance (d) and source distance (d) the binary beam shape input is most importance, due to the fact that this input mask is the only one providing the network with information about the beam position and orientation concerning shape and limits

ct and radiological depth provide structural information about the patient anatomy. the radiological depth in particular helps the network to understand spatial dimensions when being given patches for training, because the information where a specific voxel is located inside the patient's anatomy would be lost when training with patches without the radiological depth. the algorithm for radiological depth calculation is implemented in python and based on [32]

all input masks are limited to the volume where the ct mask has a hounsfield unit value higher than 150, since this is the threshold of our institutional dose estimation software.

The entire network and training algorithm is programmed in PyTorch. The dataloading was inspired by TorchIO, a library for efficient dataloading for 3d medical imaging and especially patch based loading of 3d data. (torch io citen [33]) Due to the immense memory usage of (nummer an segmenten angeben) segments, not all segments could be loaded simultaneously into the memory. to achieve a randomised set of patches presented to the network at each training iteration, the dataloading is based on a subset of patient segments randomly selected from the entire training data pool. To further improve dataloading time, a simultaneous loading of multiple segments at the same time using multi threading was implemented.

(referenz auf bild was dataloading verdeutlicht) shows the schematic process of preloading a data queue from which random patches are taken for each batch presented to the network for training. when the queue gets filled with patches a by the user specified number of segments gets randomly selected from the pool. then another by the user specified number of random patch positions per segment are extracted from the entire volume. then the entire queue gets shuffled and is then emptied during the training process. after the dataqueue is empty it is refilled with new patches from not previously used segments. after all segments have been used for patch extraction, the list of available segments is reset.

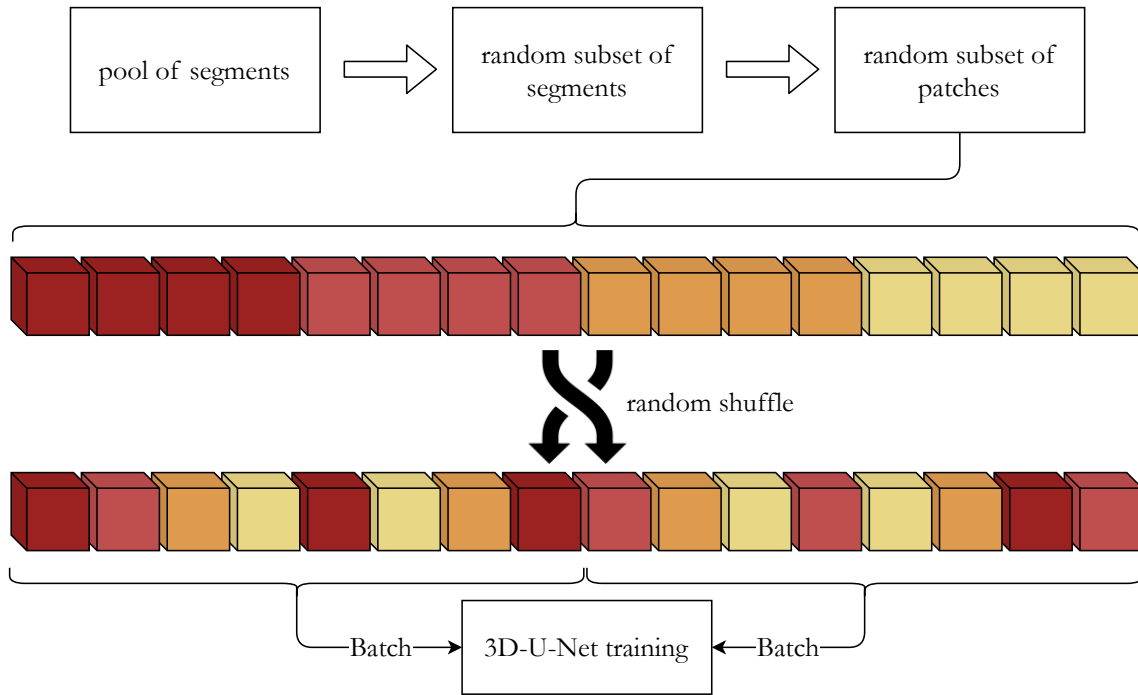


Figure 5.8: Dataloading scheme

Training

The 3D-UNet was trained on a HPC cloud based solution using a 4 Nvidia GTX 2080 Ti with 11GB of VRAM. The batchsize for training was 128 and the patch size was 32 in all dimensions resulting in the input shape of (128, 5, 32, 32, 32). Since 4 graphics cards were used each card processed 32 patches of size (5, 32, 32, 32) simultaneously. The spatial resolution of a 32 x 32 x 32 patch was 37.4 x 37.4 x 96 mm³ with voxel dimensionality of 1.17 x 1.17 x 3 mm³. The loss function used was the root mean squared error and the ADAM optimizer with a starting learning rate of 10⁻⁴, and the standard settings for beta1, beta2 and epsilon of 0.9, 0.999 and 10-8 respectively. Learning rate was reduced by a factor of 10 when no improvement in the validation loss could be observed. A validation step was done after the training queue has been refilled resulting in a validation step after 12800 patches with 64 segments per queue and 200 patches per segment. The overall accuracy regarding the 3mm/3% gamma values was assessed every 5 queue refillings. Training was stopped when no validation loss improvement could be observed for 30 epochs after learning rate reduction to 10⁻⁶.

Training supervision was done using Tensorboard in which training loss, validation loss and a the gamma pass rate could be viewed during training.

Output analysis

To assess the overall performance of the network a gamma anlysis (cite gamma paper) was perfomed. The settings for individual segments and total plan are shown in Table 5.1.

Table 5.1 Settings used for gamma analysis of single segments and entire radiation plans.

	percentage threshold /%	distance threshold /mm	lower cutoff /%	local gamma /1
segment	3 / 2 / 1	3 / 2 / 1	10	False
plan	3 / 2 / 1	3 / 2 / 1	40	False

Hier mal noch mit den anderen diskutieren, was man noch machen könnte. DVH? oder sonstige analysen der Dosis. z.B. diese Dice analyse die ich geplant hatte, wo man einen Threshold setzt und dann schauen wie sehr sich die prozente überschneiden.

Testing

The model tested on only prostate patients was tested against all other entities so assess the translational capabilities of a model only trained on one entity. The model trained on prostate, liver, breast and head and neck radio treatment data, was evaluated on all entities trained on aswell as on lypmh nodes to asses the translation to a tumor entity which was not present in the training data.

Results

Lorem ipsum dolor sit amet, consetetur sadipscing elitr, sed diam nonumy eirmod tempor invidunt ut labore et dolore magna aliquyam erat, sed diam voluptua. At vero eos et accusam et justo duo dolores et ea rebum. Stet clita kasd gubergren, no sea takimata sanctus est Lorem ipsum dolor sit amet. Lorem ipsum dolor sit amet, consetetur sadipscing elitr, sed diam nonumy eirmod tempor invidunt ut labore et dolore magna aliquyam erat, sed diam voluptua. At vero eos et accusam et justo duo dolores et ea rebum. Stet clita kasd gubergren, no sea takimata sanctus est Lorem ipsum dolor sit amet.

Discussion

Lorem ipsum dolor sit amet, consetetur sadipscing elitr, sed diam nonumy eirmod tempor invidunt ut labore et dolore magna aliquyam erat, sed diam voluptua. At vero eos et accusam et justo duo dolores et ea rebum. Stet clita kasd gubergren, no sea takimata sanctus est Lorem ipsum dolor sit amet. Lorem ipsum dolor sit amet, consetetur sadipscing elitr, sed diam nonumy eirmod tempor invidunt ut labore et dolore magna aliquyam erat, sed diam voluptua. At vero eos et accusam et justo duo dolores et ea rebum. Stet clita kasd gubergren, no sea takimata sanctus est Lorem ipsum dolor sit amet.

Conclusion

Lorem ipsum dolor sit amet, consetetur sadipscing elitr, sed diam nonumy eirmod tempor invidunt ut labore et dolore magna aliquyam erat, sed diam voluptua. At vero eos et accusam et justo duo dolores et ea rebum. Stet clita kasd gubergren, no sea takimata sanctus est Lorem ipsum dolor sit amet. Lorem ipsum dolor sit amet, consetetur sadipscing elitr, sed diam nonumy eirmod tempor invidunt ut labore et dolore magna aliquyam erat, sed diam voluptua. At vero eos et accusam et justo duo dolores et ea rebum. Stet clita kasd gubergren, no sea takimata sanctus est Lorem ipsum dolor sit amet.

Bibliography

- [1] Hans Geinitz et al. “3D conformal radiation therapy for prostate cancer in elderly patients”. In: *Radiotherapy and Oncology* 76.1 (July 2005), pp. 27–34. ISSN: 01678140. DOI: 10.1016/j.radonc.2005.06.001. URL: <https://linkinghub.elsevier.com/retrieve/pii/S0167814005002082> (visited on 08/16/2021).
- [2] Tan Dat Nguyen et al. “The curative role of radiotherapy in adenocarcinoma of the prostate in patients under 55 years of age: A rare cancer network retrospective study”. In: *Radiotherapy and Oncology* 77.3 (Dec. 2005), pp. 286–289. ISSN: 01678140. DOI: 10.1016/j.radonc.2005.10.015. URL: <https://linkinghub.elsevier.com/retrieve/pii/S0167814005004779> (visited on 08/16/2021).
- [3] Tom Budiharto, Karin Haustermans, and Gyoergy Kovacs. “External Beam Radiotherapy for Prostate Cancer”. In: *Journal of Endourology* (), p. 10.
- [4] Joseph Ragaz et al. “Adjuvant Radiotherapy and Chemotherapy in Node-Positive Premenopausal Women with Breast Cancer”. In: *The New England Journal of Medicine* (1997), p. 7.
- [5] Mario De Lena et al. “Combined Chemotherapy-Radiotherapy Approach in Locally Advanced (T3b-T4) Breast Cancer”. In: (), p. 7.
- [6] Carolyn Taylor et al. “Estimating the Risks of Breast Cancer Radiotherapy: Evidence From Modern Radiation Doses to the Lungs and Heart and From Previous Randomized Trials”. In: *Journal of Clinical Oncology* 35.15 (May 20, 2017), pp. 1641–1649. ISSN: 0732-183X. DOI: 10.1200/JCO.2016.72.0722. URL: <https://www.ncbi.nlm.nih.gov/pmc/articles/PMC5548226/> (visited on 08/16/2021).
- [7] N. R. Datta et al. “Head and neck cancers: Results of thermoradiotherapy versus radiotherapy”. In: *International Journal of Hyperthermia* 6.3 (Jan. 1990), pp. 479–486. ISSN: 0265-6736, 1464-5157. DOI: 10.3109/02656739009140944. URL: <http://www.tandfonline.com/doi/full/10.3109/02656739009140944> (visited on 08/16/2021).
- [8] S.A. Bhide and C.M. Nutting. “Advances in radiotherapy for head and neck cancer”. In: *Oral Oncology* 46.6 (June 2010), pp. 439–441. ISSN: 13688375. DOI: 10.1016/j.oraloncology.2010.03.005. URL: <https://linkinghub.elsevier.com/retrieve/pii/S1368837510000941> (visited on 08/16/2021).
- [9] Pierre Castadot et al. “Adaptive Radiotherapy of Head and Neck Cancer”. In: *Seminars in Radiation Oncology* 20.2 (Apr. 2010), pp. 84–93. ISSN: 10534296. DOI: 10.1016/j.semradonc.2009.11.002. URL: <https://linkinghub.elsevier.com/retrieve/pii/S1053429609000769> (visited on 08/16/2021).

- [10] Howard E. Morgan and David J. Sher. “Adaptive radiotherapy for head and neck cancer”. In: *Cancers of the Head & Neck* 5.1 (Dec. 2020), p. 1. ISSN: 2059-7347. DOI: 10.1186/s41199-019-0046-z. URL: <https://cancersheadneck.biomedcentral.com/articles/10.1186/s41199-019-0046-z> (visited on 08/16/2021).
- [11] Morten Høyer et al. “Radiotherapy for Liver Metastases: A Review of Evidence”. In: *International Journal of Radiation Oncology*Biophysics* 82.3 (Mar. 1, 2012), pp. 1047–1057. ISSN: 0360-3016. DOI: 10.1016/j.ijrobp.2011.07.020. URL: <https://www.sciencedirect.com/science/article/pii/S0360301611030902> (visited on 08/16/2021).
- [12] Jörn Wulf et al. “Stereotactic Radiotherapy of Targets in the Lung and Liver:” in: *Strahlentherapie und Onkologie* 177.12 (Dec. 2001), pp. 645–655. ISSN: 0179-7158. DOI: 10.1007/PL00002379. URL: <http://link.springer.com/10.1007/PL00002379> (visited on 08/16/2021).
- [13] Joern Wulf et al. “Stereotactic radiotherapy of primary liver cancer and hepatic metastases”. In: *Acta Oncologica* 45.7 (Jan. 2006), pp. 838–847. ISSN: 0284-186X, 1651-226X. DOI: 10.1080/02841860600904821. URL: <http://www.tandfonline.com/doi/full/10.1080/02841860600904821> (visited on 08/16/2021).
- [14] Florian Sterzing et al. “Stereotactic body radiotherapy for liver tumors: Principles and practical guidelines of the DEGRO Working Group on Stereotactic Radiotherapy”. In: *Strahlentherapie und Onkologie* 190.10 (Oct. 2014), pp. 872–881. ISSN: 0179-7158, 1439-099X. DOI: 10.1007/s00066-014-0714-1. URL: <http://link.springer.com/10.1007/s00066-014-0714-1> (visited on 08/16/2021).
- [15] Jacob S Witt, Stephen A Rosenberg, and Michael F Bassetti. “MRI-guided adaptive radiotherapy for liver tumours: visualising the future”. In: *The Lancet Oncology* 21.2 (Feb. 1, 2020), e74–e82. ISSN: 1470-2045. DOI: 10.1016/S1470-2045(20)30034-6. URL: <https://www.sciencedirect.com/science/article/pii/S1470204520300346> (visited on 08/16/2021).
- [16] Breast Cancer Expert Panel of the German Society of Radiation Oncology (DEGRO) et al. “DEGRO practical guidelines for radiotherapy of breast cancer IV: Radiotherapy following mastectomy for invasive breast cancer”. In: *Strahlentherapie und Onkologie* 190.8 (Aug. 2014), pp. 705–714. ISSN: 0179-7158, 1439-099X. DOI: 10.1007/s00066-014-0687-0. URL: <http://link.springer.com/10.1007/s00066-014-0687-0> (visited on 08/16/2021).
- [17] Haruo Matsushita et al. “Stereotactic Radiotherapy for Oligometastases in Lymph Nodes—A Review”. In: *Technology in Cancer Research & Treatment* 17 (Jan. 2018), p. 153303381880359. ISSN: 1533-0346, 1533-0338. DOI: 10.1177/1533033818803597. URL: <http://journals.sagepub.com/doi/10.1177/1533033818803597> (visited on 08/16/2021).

- [18] John L. Mikell et al. "Postoperative Radiotherapy is Associated with Better Survival in Non-Small Cell Lung Cancer with Involved N2 Lymph Nodes: Results of an Analysis of the National Cancer Data Base". In: *Journal of Thoracic Oncology* 10.3 (Mar. 2015), pp. 462–471. ISSN: 15560864. DOI: 10.1097/JTO.0000000000000411. URL: <https://linkinghub.elsevier.com/retrieve/pii/S1556086415316543> (visited on 08/16/2021).
- [19] Dan Lundstedt et al. "Long-term symptoms after radiotherapy of supraclavicular lymph nodes in breast cancer patients". In: *Radiotherapy and Oncology* 103.2 (May 2012), pp. 155–160. ISSN: 01678140. DOI: 10.1016/j.radonc.2011.12.017. URL: <https://linkinghub.elsevier.com/retrieve/pii/S0167814011007572> (visited on 08/16/2021).
- [20] Barbara Alicja Jereczek-Fossa, Sara Ronchi, and Roberto Orecchia. "Is Stereotactic Body Radiotherapy (SBRT) in lymph node oligometastatic patients feasible and effective?" In: *Reports of Practical Oncology and Radiotherapy* 20.6 (2015), pp. 472–483. ISSN: 1507-1367. DOI: 10.1016/j.rpor.2014.10.004. URL: <https://www.ncbi.nlm.nih.gov/pmc/articles/PMC4661354/> (visited on 08/16/2021).
- [21] Samaneh Kazemifar et al. "Segmentation of the prostate and organs at risk in male pelvic CT images using deep learning". In: *Biomedical Physics & Engineering Express* 4.5 (July 23, 2018), p. 055003. ISSN: 2057-1976. DOI: 10.1088/2057-1976/aad100. URL: <https://iopscience.iop.org/article/10.1088/2057-1976/aad100> (visited on 08/23/2021).
- [22] Shujun Liang et al. "Deep-learning-based detection and segmentation of organs at risk in nasopharyngeal carcinoma computed tomographic images for radiotherapy planning". In: *European Radiology* 29.4 (Apr. 2019), pp. 1961–1967. ISSN: 0938-7994, 1432-1084. DOI: 10.1007/s00330-018-5748-9. URL: <http://link.springer.com/10.1007/s00330-018-5748-9> (visited on 08/23/2021).
- [23] Dinggang Shen et al., eds. *Medical Image Computing and Computer Assisted Intervention – MICCAI 2019: 22nd International Conference, Shenzhen, China, October 13–17, 2019, Proceedings, Part II*. Vol. 11765. Lecture Notes in Computer Science. Cham: Springer International Publishing, 2019. ISBN: 978-3-030-32244-1 978-3-030-32245-8. DOI: 10.1007/978-3-030-32245-8. URL: <https://link.springer.com/10.1007/978-3-030-32245-8> (visited on 08/23/2021).
- [24] Jiawei Fan et al. "Automatic treatment planning based on three-dimensional dose distribution predicted from deep learning technique". In: *Medical Physics* 46.1 (Jan. 2019), pp. 370–381. ISSN: 00942405. DOI: 10.1002/mp.13271. URL: <http://doi.wiley.com/10.1002/mp.13271> (visited on 03/16/2021).
- [25] Zhiqiang Liu et al. "A deep learning method for prediction of three-dimensional dose distribution of helical tomotherapy". In: *Medical Physics* 46.5 (May 2019), pp. 1972–1983. ISSN: 0094-2405, 2473-4209. DOI: 10.1002/mp.13490. URL: <https://onlinelibrary.wiley.com/doi/abs/10.1002/mp.13490> (visited on 03/16/2021).

- [26] C. Kontaxis et al. “DeepDose: Towards a fast dose calculation engine for radiation therapy using deep learning”. In: *Physics in Medicine & Biology* 65.7 (Apr. 2020). Publisher: IOP Publishing, p. 075013. ISSN: 0031-9155. DOI: 10.1088/1361-6560/ab7630. URL: <https://doi.org/10.1088/1361-6560/ab7630> (visited on 08/23/2021).
- [27] Ti Bai et al. “Deep dose plugin: towards real-time Monte Carlo dose calculation through a deep learning-based denoising algorithm”. In: *Machine Learning: Science and Technology* 2.2 (June 1, 2021), p. 025033. ISSN: 2632-2153. DOI: 10.1088/2632-2153/abdbfe. URL: <https://iopscience.iop.org/article/10.1088/2632-2153/abdbfe> (visited on 08/23/2021).
- [28] Xiao Han. “MR-based synthetic CT generation using a deep convolutional neural network method”. In: *Medical Physics* 44.4 (2017). _eprint: <https://aapm.onlinelibrary.wiley.com/doi/abs/10.1002/mp.12155> pp. 1408–1419. ISSN: 2473-4209. DOI: 10.1002/mp.12155. URL: <https://aapm.onlinelibrary.wiley.com/doi/abs/10.1002/mp.12155> (visited on 08/23/2021).
- [29] Jelmer M. Wolterink et al. “Deep MR to CT Synthesis Using Unpaired Data”. In: *Simulation and Synthesis in Medical Imaging*. Ed. by Sotirios A. Tsaftaris et al. Lecture Notes in Computer Science. Cham: Springer International Publishing, 2017, pp. 14–23. ISBN: 978-3-319-68127-6. DOI: 10.1007/978-3-319-68127-6_2.
- [30] Anna M. Dinkla et al. “MR-Only Brain Radiation Therapy: Dosimetric Evaluation of Synthetic CTs Generated by a Dilated Convolutional Neural Network”. In: *International Journal of Radiation Oncology*Biophysics* 102.4 (Nov. 2018), pp. 801–812. ISSN: 03603016. DOI: 10.1016/j.ijrobp.2018.05.058. URL: <https://linkinghub.elsevier.com/retrieve/pii/S0360301618309106> (visited on 08/23/2021).
- [31] *nrc-cnrc/EGSnrc*. original-date: 2012-11-28T19:26:41Z. Aug. 7, 2021. URL: <https://github.com/nrc-cnrc/EGSnrc> (visited on 08/17/2021).
- [32] R. L. Siddon. “Fast calculation of the exact radiological path for a three-dimensional CT array”. In: *Medical Physics* 12.2 (Apr. 1985), pp. 252–255. ISSN: 0094-2405. DOI: 10.1118/1.595715.
- [33] Fernando Pérez-García, Rachel Sparks, and Sébastien Ourselin. “TorchIO: A Python library for efficient loading, preprocessing, augmentation and patch-based sampling of medical images in deep learning”. In: *Computer Methods and Programs in Biomedicine* 208 (Sept. 1, 2021), p. 106236. ISSN: 0169-2607. DOI: 10.1016/j.cmpb.2021.106236. URL: <https://www.sciencedirect.com/science/article/pii/S0169260721003102> (visited on 08/17/2021).

Appendix Title

Lorem ipsum dolor sit amet, consetetur sadipscing elitr, sed diam nonumy eirmod tempor invidunt ut labore et dolore magna aliquyam erat, sed diam voluptua. At vero eos et accusam et justo duo dolores et ea rebum. Stet clita kasd gubergren, no sea takimata sanctus est Lorem ipsum dolor sit amet. Lorem ipsum dolor sit amet, consetetur sadipscing elitr, sed diam nonumy eirmod tempor invidunt ut labore et dolore magna aliquyam erat, sed diam voluptua. At vero eos et accusam et justo duo dolores et ea rebum. Stet clita kasd gubergren, no sea takimata sanctus est Lorem ipsum dolor sit amet.